Int. J. Ion Mobil. Spec.
DOI 10.1007/s12127-016-0201-8

ORIGINAL RESEARCH

Towards the analysis of high molecular weight proteins and protein complexes using TIMS-MS

Paolo Benigni[1] · Rebecca Marin[1] · Juan Camilo Molano-Arevalo[1] · Alyssa Garabedian[1] · Jeremy J. Wolff[2] · Mark E. Ridgeway[2] · Melvin A. Park[2] · Francisco Fernandez-Lima[1,3]

Received: 13 May 2016 / Revised: 26 May 2016 / Accepted: 29 May 2016

Abstract In the present work, we demonstrate the potential and versatility of TIMS for the analysis of proteins, DNA-protein complexes and protein-protein complexes in their native and denatured states. In addition, we show that accurate CCS measurement are possible using internal and external mobility calibration and in good agreement with previously reported CCS values using other IMS analyzers (<5 % difference). The main challenges for the TIMS-MS analysis of high mass proteins and protein complexes in the mobility and *m/z* domain are described. That is, the analysis of high molecular weight systems in their native state may require the use of higher electric fields or a small compromise in the TIMS mobility resolution by reducing the bath gas velocity in order to effectively trap at lower electric fields. This is the first report of CCS measurements of high molecular weight biomolecules and biomolecular complexes (~150 kDa) using TIMS-MS.

Keywords TIMS · IMS-MS · Ion mobility spectrometry – mass spectrometry · Proteins · Ion—neutral collision cross sections

Introduction

Experimental determination of biomolecular structures remains a challenging problem despite recent developments in theoretical approaches that are based on available experimental structural observations (e.g., *ab initio*, molecular dynamics and bioinformatics-based prediction strategies) [1]. The elucidation of structural features of interest for biomolecules and biomolecular complexes is challenging because of the highly heterogeneous and dynamic character of biomolecules and their low relative concentrations within physiologically relevant conditions [2–11]. While X-ray crystallography and NMR spectroscopy excel at revealing structures of molecules at the atomic level, these approaches are limited by the fact that they often describes a single state of the biomolecule and/or biomolecular complex structure [12–17]. Moreover, since neither technology involves component separation during analysis, both require highly purified samples [18, 19].

Recent innovations in speed, accuracy, and sensitivity have established mass spectrometry (MS) based methods as a key technology within the field of structural biology [20]. Specifically native MS techniques, which have been developed over the last two decades, permits the structural interrogation of intact biomolecules and biomolecular complexes at biologically relevant conditions, which are not accessible by other methods [21–25]. Attention has been drawn towards the characterization of intrinsically disordered proteins (IDP) [26–28], antibody therapeutics [29–32], and even massive protein complexes [33–37] that cannot be studied using traditional structural techniques. Most common gas-phase structural probing is based on, or a combination of, tandem MS (ergodic and non-ergodic), gas-phase hydrogen-deuterium exchange, ion spectroscopy, and ion mobility spectrometry.

In particular, ion mobility spectrometry (IMS) is based on the separation of ions as they drift in a bath of inert neutral molecules under the influence of a weak electric field [38–40]. The ion's mobility gives information on their size and shape via the momentum transfer ion-neutral collision cross section (CCS) [41]. This description holds true for most contemporary

✉ Francisco Fernandez-Lima
fernandf@fiu.edu

[1] Department of Chemistry & Biochemistry, Florida International University, 11200 SW 8th St AHC4-233, Miami, FL 33199, USA

[2] Bruker Daltonics, Inc., Billerica, MA 01821, USA

[3] Biomolecular Science Institute, Florida International University, Miami, FL 33199, USA

Published online: 07 June 2016

IMS analyzers (e.g., periodic focusing DC ion guide [42–44], segmented quadrupole drift cell [45], multistage IMS [46–48], traveling wave ion guide (TWIMS) [49, 50], and SLIM devices [51]), and a common pursuit has been to increase IMS resolving power and ion transmission [52–60]. Many different forms of IMS have been used in the analysis of biological molecules for the analysis of isotopomers [61], proteins [62, 63], protein complexes [64–71], folding pathways [72–74], unstructured/intrinsically disordered proteins [75–79], as well as collisionally activated states of peptides and proteins [69, 80–87]. It should be noted that, in the case of structural biology, gas-phase studies take advantage of the desolvation process to effectively reduce sample complexity, permitting molecular characterization in the absence of bulk solvent.

With the recent introduction of a new IMS analyzer - Trapped Ion Mobility Spectrometer (TIMS)- the possibility to decouple the time domain from the IMS separation allows for the study of conformationally trapped molecular ions in the gas-phase as a function of the desolvation time, temperature and bath gas composition. TIMS' mode of operation and its advantages over traditional IMS are described in ref [88–90]. We have shown the use of TIMS for the study of isomerization kinetics of small molecules [91], peptides [92], and proteins [19, 93–95], the influence of the collision partner on the molecular structure [96], and the factors that affect molecular-adduct complex lifetime and stability during TIMS measurements [97]. In particular, we have shown the combination of simultaneous measurement of first principle derived collision cross sections and back-exchange HDX rates using a TIMS device with theoretical calculations for the assignment of candidate structures of kinetic intermediates as a way to study folding/unfolding pathways [92].

In this work, we further investigate the potential of trapped ion mobility spectrometry (TIMS) for the separation and characterization of high molecular weight proteins and protein complexes. In particular, the discussion is based on the fundamental factors that affect the molecular ion trapping of high mass molecular systems, the collision cross section calculations and the differences between native and non-native states.

Experimental methods

Material and reagents

Most proteins utilized in this study were purchased (e.g., ubiquitin, equine holomyoglobin, carbonic anhydrase from bovine erythrocytes, β-lactoglobulin, equine cytochrome C, and bovine serum albumin) from Sigma-Aldrich (St. Louis, MO, USA), or provided by collaborators (e.g., Avastin, HMGA2 [98], rat Calmodulin [99] and recombinant mouse DREAM [93]) and used as received. DNA sequences FL875(CCCCCCATATT CGCGATTATTGCCCCCGCAATAATCG CGAATAT GGGGGG), FL876 (GGATATTGCCCCCGCAATATCC) were purchased from Eurofin (Ebersberg, Germany). Protein solutions were prepared at a final 1–10 μM concentration in 10–100 mM ammonium acetate, 0–50 % methanol, and 0–10 % acetic acid. Low concentration Tuning Mix (G2421A; Agilent Technologies, Santa Clara, CA, USA) was used as a mobility calibration standard. All solvents and ammonium acetate salts used in these studies were analytical grade or better and purchased from Fisher Scientific (Pittsburg, PA, USA).

TIMS-MS analysis

Details regarding the TIMS operation and specifics compared to traditional IMS can be found elsewhere [88–92]. Briefly, mobility separation in TIMS is based on holding the ions stationary using an electric field against a moving gas. The separation in a TIMS device can be described by the center of the mass frame using the same principles as in a conventional IMS drift tube [41]. Since mobility separation is related to the number of ion-neutral collisions (or drift time in traditional drift tube cells), the mobility separation in a TIMS device depends on the bath gas drift velocity, ion confinement and ion elution parameters. The mobility in a TIMS analyzer can be described as:

$$K_i = \upsilon_g / E_x(i) = A(1/(V_{out}\text{-}V_{elu}(i))) \quad (1)$$

where υ_g is the velocity of the bath gas in the mobility cell and $E_x(i)$ is the electric field at which the specific packet of ions elute. These parameters can be related to the elution voltage ($V_{elu}(i)$) and the exit voltage (V_{out}) of the region exit. The calibration constant A was determined from previously reported mobility values for Tuning Mix calibration standard (G24221A, Agilent Technologies, Santa Clara, CA) in nitrogen ($m/z = 322$, $K_0 = 1.376$ cm^2 V^{-1} s^{-1} and $m/z = 622$, $K_0 = 1.013$ cm^2 V^{-1} s^{-1}) 90, 100]. From the mobility K value, the collisional cross section (CCS) can be determined by the following equation:

$$CCS = \frac{(18\pi)^{\frac{1}{2}}}{16} \frac{z}{(k_b T)^{\frac{1}{2}}} \left[\frac{1}{m_1} + \frac{1}{m_b}\right]^{\frac{1}{2}} \frac{1}{K} \frac{760}{P} \frac{T}{273.15} \frac{1}{N^*} \quad (2)$$

Where the charge of the ion is represented by z, k_b represents the Boltzman constant, m_1 and m_b are the masses of molecular ion and the bath gas and N^* is the number density.

TIMS-MS operation parameters

TIMS operation can be tuned for either wide range mobility analysis, with a voltage ramp of $\Delta V_{ramp} = 200$ V, or for narrow mobility selection, with a narrow voltage ramp of $\Delta V_{ramp} = 10–30$ V. In both cases ramp times of up to 500 ms are used for analysis. Notice that TIMS mobility

resolution depends on both the ramp size as well as the ramp speed, where lower speeds give higher mobility resolutions [88–90]. In addition to the ramp speed, the velocity of the gas also defines the mobility resolution and trapping efficiency of the TIMS analyzer. Increasing the velocity of the gas, by changing the pressure difference between the front (P_1 = 1.1–4.3 mbar) and the end (P_2 = 0.6–3.0 mbar) of the analyzer region also increases the mobility resolution. As the velocity of the gas increases the ions experience a greater drag force, requiring higher electric fields in order to be trapped. A constant radiofrequency (RF) is applied to the entrance, analyzer and exit region of the TIMS analyzer (frequency of 880 kHz with 200–300 V peak-to-peak). Each funnel electrode is divided into four electrically insulated segments that are used to create a dipole field in the entrance and exit section, to focus the ions downstream, and a quadrupolar field in the separation region to radially confine the ions during the ion trapping and analysis. That is, in the entrance and exit funnel sections, the RF potential applied to the ion funnel is 180° out of phase between adjacent plates. This results in a pseudo-potential, which pushes the ions away from the funnel walls. However, in the analyzer section, the phase of the RF potential does not alternate between adjacent plates but only between adjacent segments. The purpose of the quadrupolar field in the analyzer section is to confine (trap) the ions radially and avoid ion losses due to diffusion. The TIMS analyzer was coupled to a maXis Impact QUHR-TOF (Bruker Daltonics Inc., Billerica, MA). Data acquisition was controlled using in-house software and synchronized with the maXis Impact acquisition program.

Atmospheric pressure ionization sources

Electrospray ionization source (ESI) An orthogonal, commercial ESI source based on the Apollo II design (Bruker Daltonics, Inc., MA) was used. Briefly, sample solutions were introduced into the nebulizer at a rate of 120–180 μL/min using an external syringe pump. Typical operating conditions were 4000–4500 V capillary voltage, 600 V endcap capillary offset voltage, 10 L/min dry gas flow rate, 1.0 bar nebulizer gas pressure, and a dry gas temperature 180 °C. Ions from the ESI source are introduced via a 0.6 mm inner diameter, single-bore glass capillary tube, which is resistively coated across its length, allowing the nebulizer to be maintained at ground potential, while the capillary exit was biased to around 180 V.

nanoElectrospray ionization source (nanoESI) A custom-built, pulled capillary orthogonal nanoESI source was utilized for all the experiments. Quartz glass capillaries (O.D.: 1.0 mm and I.D.: 0.70 mm) were pulled utilizing a P-2000 micropipette laser puller (Sutter Instruments, Novato, CA) and loaded with 10 μL aliquot sof the sample solution. A typical nanoESI source voltage of 600–1200 V was applied between the pulled capillary tips and the TIMS-MS instrument inlet. Ions were introduced into the TIMS cell via a stainless steel tube (1/16 × 0.020”, IDEX Health Science, Oak Harbor, WA), which was held at room temperature.

Theoretical calculations

Theoretical collisional cross sections were calculated from X-ray structures for myoglobin (pdb: 1YMB), cytochrome C (pdb: 1HRC), β-lactoglobulin (pdb:4GNY), and ubiquitin (pdb:1UBQ), and were used as is [100–103]. Ion mobilities were calculated for the X-ray structures using the trajectory method (TM) utilizing IMoS (v.106W64dsoftware [104–108]. This calculation software allows the calculation of collisional cross sections of ions using both traditional methods as well as new methods such as Diffuse Hard Sphere Scattering and Diatomic Trajectory Method. For molecules without defined partial charges the charge is centered at the center of mass of the protein. Gas particles originate from a bounding box from the x, y, and z planes and are diagonalized

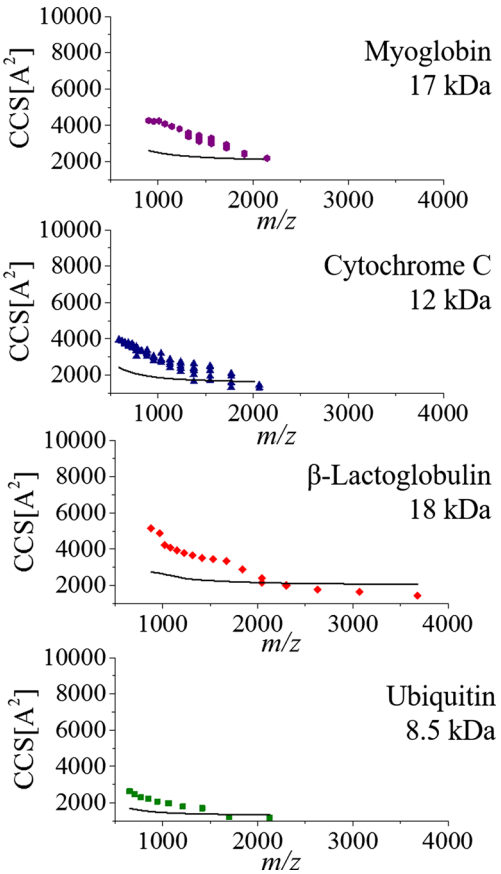

Fig. 1 Ion-neutral collisional cross section dependence on the m/z for globular proteins (myoglobin and cytochrome C) and barrel proteins (β-lactoglobulin and ubiquitin) in their native and denature states. In *black*, theoretical values obtained from reported tridimensional structures based on X-ray measurements

in order to determine the collisional cross section of the ions. Calculations were performed with 3 TM rotations, with 300, 000 gas molecules, and 92 % Maxwell distributed remission velocity. Mobility calculations were performed for all experimentally observed charge states.

Results and discussion

Ion mobility spectrometry (IMS) combined with molecular dynamic simulations has proven to be a versatile technique for the analysis of intermediate and equilibrium structures of

Table 1 Ion-neutral collisional cross sections measured by nanoESI-TIMS-MS in nitrogen as a bath gas for proteins, protein – DNA complexes and protein-protein complexes

Protein	*m/z (charge), CCS;*
Avastin	5960 (+25), 6709; 5731 (+26), 6997; 5519 (+27), 7031;
BSA dimer	5870 (+23), 6208; 5625 (+24), 6454; 5400 (+25), 6699;
BSA	4467 (+15), 4200, 4188 (+16), 4291, 3941 (+17), 4351; 3722 (+18), 4476;
β-Lactoglobulin dimer	2831 (+13), 3430;
DREAM*	2455 (+12), 3025, 3181; 2266 (+13), 3561, 3756, 4078; 2104 (+14), 4029, 4195, 4315, 4526; 1964 (+15), 4243, 4459, 4809; 1841 (+16), 4526, 4829, 5024; 1733 (+17), 4663, 4829, 5102; 1636 (+18), 4751, 5317; 1473 (+20), 5151, 5639; 1403 (+21), 5756, 5912, 6253, 6467; 1339 (+22), 5951, 6184, 6340,6526; 1281 (+23), 6223, 6585, 6818; 1227 (+24), 6760, 6917, 7062
Carbonic anhydrase	2887 (+10), 2530; 2625 (+11), 2606; 1444 (+20), 5422; 1375(+21), 5510; 1312 (+22), 5863; 1255 (+23), 6625; 1203 (+24), 6809; 1155 (+25), 6962; 1110 (+26), 7144, 1069 (+27), 7317; 1031 (+28), 7475; 996 (+29), 7596; 962 (+30), 7710; 931 (+31), 7831; 902 (+32), 7943; 875 (+33), 8139; 849 (+34), 8276; 825 (+35), 8380; 802 (+36), 8559; 780 (+37), 8692; 760 (+38), 8755; 740 (+39), 8906
Myoglobin	2147 (+8), 2187; 1908 (+9), 2399,2465; 1717 (+10), 2749, 2805, 2882, 2937; 1561 (+11), 2992, 3052, 3125, 3228, 3300; 1431 (+12), 3123, 3192, 3209, 3300, 3337, 3385, 3446, 3374, 3446, 3531, 3591; 1227 (+13), 3809; 1145 (+14), 3945; 1073 (+15), 4084; 1010 (+16), 4245; 954 (+16), 4222; 904 (+17), 4266
β-Lactoglobulin	3680 (+5), 1422; 3067 (+6), 1636; 2629 (+7), 1773; 2300 (+8), 1995; 2044 (+9), 2155, 2381; 1840 (+10), 2867, 1673 (+11), 3343; 1533 (+12), 3449; 1415 (+13), 3518; 1314 (+14), 3655; 1227 (+15), 3795; 1150 (+16), 3937; 1082 (+17), 4076; 1022 (+18), 4207; 968 (+19), 4867; 876 (+21), 5152
Ubiquitin	2125 (+4), 1149; 1700 (+5), 1229; 1417 (+6), 1699; 1214 (+7), 1794; 1063 (+8), 1975; 944 (+9), 2069; 850 (+10), 2213; 773 (+11), 2292; 708 (+12), 2468; 654 (+13), 2624
Cytochrome C	2064 (+6), 1289, 1438; 1769 (+7), 1307, 1574, 1922, 2083; 1548 (+8), 1686, 1925, 2249, 2468, 2496; 1376 (+9), 1637, 2024, 2258, 2358, 2388, 2631; 1238 (+10), 2181, 2365, 2508, 2652, 2717; 1125 (+11) 2403, 2553, 276, 2813, 2861; 1032 (+12), 2678, 2805, 2877, 3189; 952 (+13), 2794, 2969, 2998, 3044; 825.6 (+14), 3279, 3318, 3358; 774 (+16), 3036, 3311, 3382, 3465, 3557; 728 (+17), 3516, 3611, 3663, 3724; 688 (+18), 3598, 3689, 3743, 3778; 651 (+19), 3727, 3798; 619 (+20), 3885, 589 (+21), 3907,3954
Calmodulin	2405 (+7), 1860; 2104 (+8), 1915, 2103, 2378; 1870 (+9), 2256, 2396, 2750, 2933; 1684 (+10), 2741, 2981; 1530, (+11), 2957, 3097, 3256, 3323; 1403 (+12), 3170, 3323, 3402; 1295 (+13), 3512, 3591, 3707; 1202 (+14), 3695, 3749, 3847; 1122 (+15), 3841, 3944; 1052 (+16), 1091; 990 (+17) 4212, 935 (+18), 4341
HMGA2	1477 (+8), 2114; 1313 (+9), 2353; 1181 (+10), 2511; 1074 (+11), 2704; 984 (+12), 2869, 2890; 909 (+13), 2998; 844 (+14), 2967, 3059, 3130; 787 (+15), 3236, 3334; 739 (+16), 3339
FL876 + HMGA2 (GGATATTGCCCCCGCAATATCC)	2639 (+7), 1624; 2309 (+8), 1658; 2053 (+9), 1741, 2003; 1847 (+10), 1769, 1621, 2082, 2169, 2286; 1680 (+11), 2148, 2423; 1540 (+12), 2582, 2748; 1421 (+13), 2706, 2886; 1320 (+14), 2810, 3031, 3258; 1232 (+15), 2921, 3204; 1155 (+16), 3300, 3548; 1087 (+17) 3651, 4003;
FL875 + HMGA2 (FL875: CCCCCCATATTCGCGATTATTG CCCCCGCAATAATCGCGAATATGGGGGG)	3401 (+8), 1991; 3023 (+9), 2069; 2721 (+10), 2098, 2140, 2246, 2459

biomolecules enabling the correlation of ion-neutral, collision cross sections (CCS) with candidate structures [109–115]. In particular, it has been shown that by using soft ionization techniques (e.g., ESI) the evaporative cooling of the solvent leads to a freezing of multiple conformations, which has permitted the study of the conformational space dependence on the solvent conditions (e.g., native vs denatured), bath gas collision partner, and temperature [116, 117]. For example, changes in the starting solution conditions (e.g., pH, organic content, etc.) can induce changes in the charge state distribution and the conformational space that is accessible during the IMS-MS measurements [118–121]. In addition, changes in the conformational space can be observed as a function of the desolvation process and upon activation prior to the IMS-MS measurements. Previous work using TIMS-MS has shown the possibility to trap a wide mobility range from small molecules to small proteins [122, 123]; however, it was also demonstrated that the trapping efficiency is a function of the electrode geometry, bath gas profile and electrical confining parameters (e.g., radiofrequency value and amplitude).

Biomolecules can exist in several conformational states inside the cell and their functions are directly related to the folding/unfolding mechanism. Thus, to better understand the structural properties of biomolecules there is a need to accurately measure the CCS, which changes as a function of their conformational state. Biomolecular ions can be introduced in the TIMS analyzer in native and denatured states (see Fig. 1). The increase in charge state is generally accompanied by the observation of more denatured conformational states with higher CCS values. That is, the degree of folding/unfolding can be observed as the charge state changes, reflecting biomolecular structural changes and any major transitions. For example, in the case of globular proteins (e.g., cytochrome C 12 kDa and myoglobin 17 kDa), a change from single native state to multiple molten globule and unfolded conformational states are observed. Notice that while the CCS values agree with previously reported CCS using DT-IMS-MS and TWIMS-MS, within 5 %, the higher resolution of the TIMS permits, for the first time, the separation of a larger number of conformations. Moreover, in the case of barrel proteins (e.g., Ubiquitin 8.5 kDa and β-Lactoglobulin 18.4 kDa) in addition to the unfolding trend, abrupt changes in the CCS can be correlated to significant conformational transitions. When compared to other structural measurements (e.g., solution NMR and X-ray crystallography, solid line in Fig. 1), it can be seen that the increase in CCS with the charge state is not merely due to the charge dependence of the CCS, but a consequence of structural changes in the molecular ion (see Eq. 1). A more detailed list of CCS values as a function of the charge state is shown in Table 1 for protein, DNA-protein complexes, and protein-protein complexes using both ESI and nanoESI sources.

The charge state dependence with the CCS shows that, as the protein mass increases, there is a need to measure higher *m/z* in order to sample native conformations. Previous work has shown that with extended mass range MS analyzers, larger proteins and protein complexes can be studied by IMS-MS [124]. In the case of TIMS-MS, a similar approach can be taken but different from other IMS variants, the experimental conditions for molecular ion trapping and efficiency in the TIMS analyzer plays a major role. For example, nanoESI-TIMS-MS can separate larger molecular ions based on both mobility and *m/z* (see example in Fig. 2 for the BSA dimer 132 kDa and the Avastin monomer 149 kDa) under native conditions. However, it should be noted that the TIMS-MS experiment can be performed under multiple trapping conditions. That is, in TIMS ion trapping is based on compensating the drift force (defined by the pressured difference in the tunnel region or bath gas velocity) with an electric field (see Eq. 1). However, there are practical limitations on the value of the applicable voltage difference across the tunnel region and therefore the mobility range that can be studied (see examples in Fig. 3 for TIMS measured and for predicted K values based on other IMS techniques [50, 70]). As we mentioned before, the higher the velocity of the gas the higher the

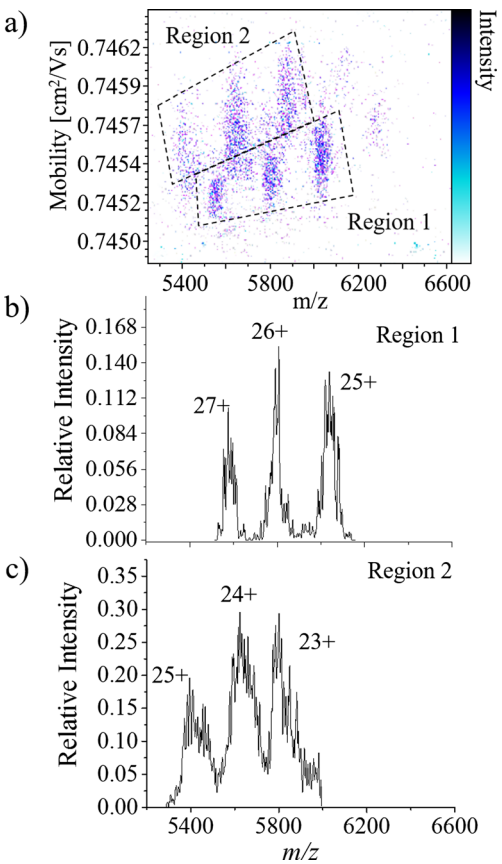

Fig. 2 **a** 2D-IMS-MS contour plot for a mixture of Avastin antibody and BSA dimer. Mass spectra projections for Region 1 (Avastin) and Region 2 (BSA dimer)

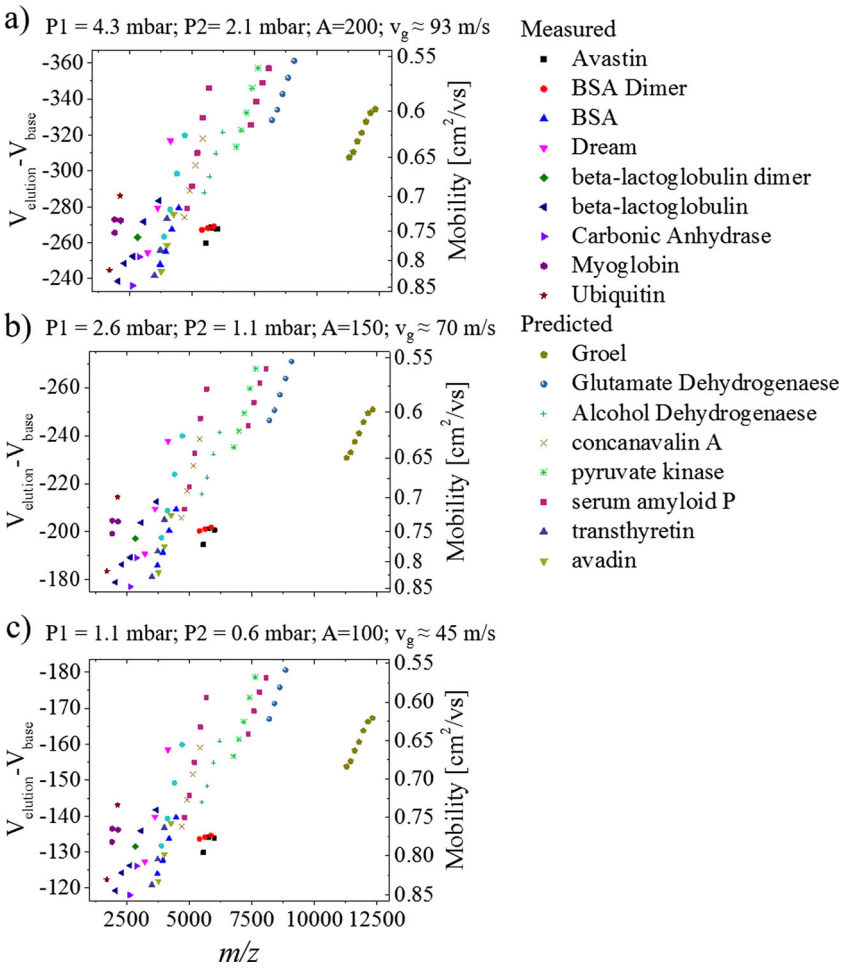

Fig. 3 Dependence of the trapping potential for a *m/z* up to 12,500 for several TIMS measured and reported biomolecular systems as a function of the bath gas velocity. Notice that as the velocity of the gas decreases, the lower the trapping potential required in the TIMS analyzer

electric field required for the analysis. For example, when TIMS-MS is operated at an A ~200 ($v_g \approx 93$ m/s), the required field strength to trap the high mass protein ions in their native state is $V_{elution}$ - $V_{base} < 360$ V. Although this electric field is technically achievably, the trapping efficiency is typically low for high mass species. Nevertheless, under these conditions, ion mobility resolutions (R = CCS/ΔCCS) of up to 400 have been achieved for lower mass systems (see example in the separation of hydroxylated polybrominated-diphenyl ethers [125]). In the case of larger mass systems, a factor of <2x in the resolving power can be compromised in order to achieved higher trapping efficiencies. For example, when TIMS-MS is operated at an A ~150 ($v_g \approx 70$ m/s) and A ~100 ($v_g \approx 45$ m/s), the required field strength to trap the high mass protein ions in their native state is $V_{elution}$ - $V_{base} < 275$ and <185 V, respectively. Under these conditions large mass proteins like glutamate dehydrogenase, and massive protein complexes, such as Groel can be analyzed. Notice that although certain proteins and protein complexes typically have a very high mass (~800 kDa for Groel), a *m/z* range of up to 12,500 will suffice to perform TIMS-MS experiments of proteins and protein complexes in their native state.

Conclusions

In the present work we demonstrate the potential and versatility of TIMS for the analysis of proteins, DNA-proteins, and protein-protein complexes in their native and denatured states. In addition, it was shown that accurate CCS measurements are possible and are in good agreement with previously reported CCS values using other IMS analyzers (<5 % difference). The main challenges for the analysis of high mass proteins and protein complexes in the mobility and *m/z* domain were described. That is, the analysis of high mass systems in their native state will require the use of higher electric fields or a compromise in the TIMS mobility resolution by reducing the bath gas velocity. This is the first report of CCS measurements of high mass biomolecules and biomolecular complexes (~150 kDa) using TIMS-MS.

Acknowledgments The authors would like to acknowledge Dr. Fenfei Leng (FIU), Dr. Jaroslava Miksovska (FIU), and Dr. Walter Gonzalez (FIU-Caltech) for their support during the protein expression, separation and purification processes, as well as Dr. Peter Sander (Bruker) for the development of DataAnalysis v. 5.0. IMoS is freely available from Dr.

Carlos Larriba-Anadaluz (UIPUI). This work was supported by National Institute of Health support (Grant No. R00GM106414 to FF-L).

References

1. Zhang Y (2008) Progress and challenges in protein structure prediction. Curr Opin Struct Biol 18(3):342–8
2. Alberts B (1998) The cell as a collection of protein machines: preparing the next generation of molecular biologists. Cell 92(3): 291–294
3. Dinant C, Luijsterburg MS, Höfer T, von Bornstaedt G, Vermeulen W, Houtsmuller AB, van Driel R (2009) Assembly of multiprotein complexes that control genome function. J Cell Biol 185(1):21–26
4. Jung E, Heller M, Sanchez J-C, Hochstrasser DF (2000) Proteomics meets cell biology: the establishment of subcellular proteomes. Electrophoresis 21(16):3369–3377
5. Hegyi H, Gerstein M (1999) The relationship between protein structure and function: a comprehensive survey with application to the yeast genome 1. J Mol Biol 288(1):147–164
6. Todd AE, Orengo CA, Thornton JM (2001) Evolution of function in protein superfamilies, from a structural perspective1. J Mol Biol 307(4):1113–1143
7. Whisstock JC, Lesk AM (2003) Prediction of protein function from protein sequence and structure. Q Rev Biophys 36(03): 307–340
8. Loo TW, Bartlett MC, Clarke DM (2003) Drug binding in human P-glycoprotein causes conformational changes in both nucleotide-binding domains. J Biol Chem 278(3):1575–1578
9. Dauber-Osguthorpe P, Roberts VA, Osguthorpe DJ, Wolff J, Genest M, Hagler AT (1988) Structure and energetics of ligand binding to proteins: escherichia coli dihydrofolate reductase-trimethoprim, a drug-receptor system. Proteins Struct Funct Bioinf 4(1):31–47
10. Teague SJ (2003) Implications of protein flexibility for drug discovery. Nat Rev Drug Discov 2(7):527–541
11. Jefferis R (2009) Recombinant antibody therapeutics: the impact of glycosylation on mechanisms of action. Trends Pharmacol Sci 30(7):356–362
12. Robinson CV, Sali A, Baumeister W (2007) The molecular sociology of the cell. Nature 450(7172):973–82
13. Sali A, Glaeser R, Earnest T, Baumeister W (2003) From words to literature in structural proteomics. Nature 422(6928):216–25
14. Ketchem RR, Lee K-C, Huo S, Cross TA. Macromolecular structural elucidation with solid-state NMR-derived orientational constraints. J Biomol NMR 8(1):1–14
15. Castellani F, van Rossum B, Diehl A, Schubert M, Rehbein K, Oschkinat H (2002) Structure of a protein determined by solid-state magic-angle-spinning NMR spectroscopy. Nature 420(6911):98–102
16. Opella SJ, Marassi FM (2004) Structure determination of membrane proteins by NMR spectroscopy. Chem Rev 104(8):3587–3606
17. Shi Y (2014) A glimpse of structural biology through x-ray crystallography. Cell 159(5):995–1014
18. Schenk ER, Nau F, Fernandez-Lima F (2015) Theoretical predictor for candidate structure assignment from IMS data of biomolecule-related conformational space. Int J Ion Mobil Spectrom 18(1–2):23–29
19. Schenk ER, Almeida R, Miksovska J, Ridgeway ME, Park MA, Fernandez-Lima F (2015) Kinetic intermediates of holo- and apomyoglobin studied using HDX-TIMS-MS and molecular dynamic simulations. J Am Soc Mass Spectrom 26(4):555–63
20. Scarff CA, Thalassinos K, Hilton GR, Scrivens JH (2008) Travelling wave ion mobility mass spectrometry studies of protein structure: biological significance and comparison with X-ray crystallography and nuclear magnetic resonance spectroscopy measurements. Rapid Commun Mass Spectrom RCM 22(20):3297–304
21. Feng X, Liu X, Luo Q, Liu BF (2008) Mass spectrometry in systems biology: an overview. Mass Spectrom Rev 27(6):635–60
22. Simoneit BR (2005) A review of current applications of mass spectrometry for biomarker/molecular tracer elucidation. Mass Spectrom Rev 24(5):719–65
23. Loo JA (1997) Studying noncovalent protein complexes by electrospray ionization mass spectrometry. Mass Spectrom Rev 16(1):1–23
24. Winston RL, Fitzgerald MC (1997) Mass spectrometry as a readout of protein structure and function. Mass Spectrom Rev 16(4): 165–179
25. Miranker A, Robinson CV, Radford SE, Aplin RT, Dobson CM (1993) Detection of transient protein folding populations by mass spectrometry. Science 262(5135):896–900
26. Dunker AK, Brown CJ, Lawson JD, Iakoucheva LM, Obradovic Z (2002) Intrinsic disorder and protein function. Biochemistry 41(21):6573–6582
27. Dunker AK, Oldfield CJ, Meng J, Romero P, Yang JY, Chen JW, Vacic V, Obradovic Z, Uversky VN (2008) The unfoldomics decade: an update on intrinsically disordered proteins. BMC Genomics 9(Suppl 2):S1
28. Dyson HJ, Wright PE (2005) Intrinsically unstructured proteins and their functions. Nat Rev Mol Cell Biol 6(3):197–208
29. Ferguson CN, Gucinski-Ruth AC (2016) Evaluation of ion mobility-mass spectrometry for comparative analysis of monoclonal antibodies. J Am Soc Mass Spectrom 27(5):822–833
30. Beck A, Sanglier-Cianférani S, Van Dorsselaer A (2012) Biosimilar, biobetter, and next generation antibody characterization by mass spectrometry. Anal Chem 84(11):4637–4646
31. Burkitt W, Domann P, O'Connor G (2010) Conformational changes in oxidatively stressed monoclonal antibodies studied by hydrogen exchange mass spectrometry. Protein Sci 19(4):826–835
32. Marcoux J, Champion T, Colas O, Wagner-Rousset E, Corvaïa N, Van Dorsselaer A, Beck A, Cianférani S (2015) Native mass spectrometry and ion mobility characterization of trastuzumab emtansine, a lysine-linked antibody drug conjugate. Protein Sci 24(8):1210–1223
33. Percipalle P, Fomproix N, Cavellán E, Voit R, Reimer G, Krüger T, Thyberg J, Scheer U, Grummt I, Östlund Farrants AK (2006) The chromatin remodelling complex WSTF–SNF2h interacts with nuclear myosin 1 and has a role in RNA polymerase I transcription. EMBO Rep 7(5):525–530
34. Kasten MM, Dorland S, Stillman DJ (1997) A large protein complex containing the yeast Sin3p and Rpd3p transcriptional regulators. Mol Cell Biol 17(8):4852–4858
35. Fischle W, Dequiedt F, Hendzel MJ, Guenther MG, Lazar MA, Voelter W, Verdin E (2002) Enzymatic activity associated with class II HDACs is dependent on a multiprotein complex containing HDAC3 and SMRT/N-CoR. Mol Cell 9(1):45–57
36. Trip EN, Scheffers D-J (2015) A 1 MDa protein complex containing critical components of the escherichia coli divisome. Sci Rep 5:18190
37. Kaplan M, Cukkemane A, van Zundert GCP, Narasimhan S, Daniels M, Mance D, Waksman G, Bonvin AMJJ, Fronzes R, Folkers GE, Baldus M (2015) Probing a cell-embedded megadalton protein complex by DNP-supported solid-state NMR. Nat Methods 12(7):649–652
38. Kanu AB, Dwivedi P, Tam M, Matz L, Hill HH Jr (2008) Ion mobility-mass spectrometry. J Mass Spectrom 43(1):1–22

39. Maurer MM, Donohoe GC, Valentine SJ (2015) Advances in ion mobility-mass spectrometry instrumentation and techniques for characterizing structural heterogeneity. Analyst 140(20):6782–98
40. Wyttenbach T, Pierson NA, Clemmer DE, Bowers MT (2014) Ion mobility analysis of molecular dynamics. Annu Rev Phys Chem 65:175–96
41. McDaniel EW, Mason EA (1973) Mobility and diffusion of ions in gases, vol 381. Wiley, New York
42. Gillig KJ, Russell DH (2001) A periodic field focusing ion mobility spectrometer. The Texas A & M University System 36
43. Gillig KJ, Ruotolo BT, Stone EG, Russell DH (2004) An electrostatic focusing ion guide for ion mobility-mass spectrometry. Int J Mass Spectrom 239(1):43–49
44. Silveira JA, Gamage CM, Blase RC, Russell DH (2010) Gas-phase ion dynamics in a periodic-focusing DC ion guide. Int J Mass Spectrom 296(1–3):36–42
45. Guo Y, Wang J, Javahery G, Thomson BA, Siu KW (2005) Ion mobility spectrometer with radial collisional focusing. Anal Chem 77(1):266–75
46. Koeniger SL, Merenbloom SI, Valentine SJ, Jarrold MF, Udseth HR, Smith RD, Clemmer DE (2006) An IMS-IMS analogue of MS-MS. Anal Chem 78(12):4161–74
47. Kurulugama RT, Nachtigall FM, Lee S, Valentine SJ, Clemmer DE (2009) Overtone mobility spectrometry: part 1. Experimental observations. J Am Soc Mass Spectrom 20(5):729–37
48. Glaskin RS, Valentine SJ, Clemmer DE (2010) A scanning frequency mode for ion cyclotron mobility spectrometry. Anal Chem 82(19):8266–71
49. Pringle SD, Giles K, Wildgoose JL, Williams JP, Slade SE, Thalassinos K, Bateman RH, Bowers MT, Scrivens JH (2007) An investigation of the mobility separation of some peptide and protein ions using a new hybrid quadrupole/travelling wave IMS/oa-ToF instrument. Int J Mass Spectrom 261(1):1–12
50. Bush MF, Hall Z, Giles K, Hoyes J, Robinson CV, Ruotolo BT (2010) Collision cross sections of proteins and their complexes: a calibration framework and database for gas-phase structural biology. Anal Chem 82(22):9557–9565
51. Webb IK, Garimella SV, Tolmachev AV, Chen TC, Zhang X, Norheim RV, Prost SA, LaMarche B, Anderson GA, Ibrahim YM, Smith RD (2014) Experimental evaluation and optimization of structures for lossless ion manipulations for ion mobility spectrometry with time-of-flight mass spectrometry. Anal Chem 86(18):9169–76
52. Dugourd P, Hudgins RR, Clemmer DE, Jarrold MF (1997) High-resolution ion mobility measurements. Rev Sci Instrum 68(2):1122–1129
53. Merenbloom SI, Glaskin RS, Henson ZB, Clemmer DE (2009) High-resolution ion cyclotron mobility spectrometry. Anal Chem 81(4):1482–7
54. Kemper PR, Dupuis NF, Bowers MT (2009) A new, higher resolution, ion mobility mass spectrometer. Int J Mass Spectrom 287(1–3):46–57
55. Blase RC, Silveira JA, Gillig KJ, Gamage CM, Russell DH (2011) Increased ion transmission in IMS: a high resolution, periodic-focusing DC ion guide ion mobility spectrometer. Int J Mass Spectrom 301(1–3):166–173
56. May JC, Russell DH (2011) A mass-selective variable-temperature drift tube ion mobility-mass spectrometer for temperature dependent ion mobility studies. J Am Soc Mass Spectrom 22(7):1134–45
57. Kemper PR, Bowers MT (1990) A hybrid double-focusing mass spectrometer—high-pressure drift reaction cell to study thermal energy reactions of mass-selected ions. J Am Soc Mass Spectrom 1(3):197–207
58. Wu C, Siems WF, Asbury GR, Hill HH (1998) Electrospray ionization high-resolution ion mobility spectrometry-mass spectrometry. Anal Chem 70(23):4929–38
59. Liu Y, Clemmer DE (1997) Characterizing oligosaccharides using injected-ion mobility/mass spectrometry. Anal Chem 69(13):2504–9
60. Jarrold MF, Constant VA (1991) Silicon cluster ions: evidence for a structural transition. Phys Rev Lett 67(21):2994–2997
61. Kaszycki JL, Bowman AP, Shvartsburg AA (2016) Ion mobility separation of peptide isotopomers. J Am Soc Mass Spectrom 27(5):795–799
62. Hogan CJ, Mora JF (2011) Ion mobility measurements of nondenatured 12–150 kDa proteins and protein multimers by Tandem Differential Mobility Analysis–Mass Spectrometry (DMA-MS). J Am Soc Mass Spectrom 22(1):158–172
63. de la Mora JF, Ude S, Thomson BA (2006) The potential of differential mobility analysis coupled to MS for the study of very large singly and multiply charged proteins and protein complexes in the gas phase. Biotechnol J 1(9):988–997
64. Duijn E v, Barendregt A, Synowsky S, Versluis C, Heck AJR (2009) Chaperonin complexes monitored by ion mobility mass spectrometry. J Am Chem Soc 131(4):1452–1459
65. Uetrecht C, Barbu IM, Shoemaker GK, van Duijn E, HeckAlbert JR (2011) Interrogating viral capsid assembly with ion mobility–mass spectrometry. Nat Chem 3(2):126–132
66. Wang SC, Politis A, Di Bartolo N, Bavro VN, Tucker SJ, Booth PJ, Barrera NP, Robinson CV (2010) Ion mobility mass spectrometry of two tetrameric membrane protein complexes reveals compact structures and differences in stability and packing. J Am Chem Soc 132(44):15468–15470
67. Uetrecht C, Rose RJ, van Duijn E, Lorenzen K, Heck AJR (2010) Ion mobility mass spectrometry of proteins and protein assemblies. Chem Soc Rev 39(5):1633–1655
68. Politis A, Park AY, Hyung S-J, Barsky D, Ruotolo BT, Robinson CV (2010) Integrating ion mobility mass spectrometry with molecular modelling to determine the architecture of multiprotein complexes. PLoS One 5(8):e12080
69. Hyung S-J, Robinson CV, Ruotolo BT (2009) Gas-phase unfolding and disassembly reveals stability differences in ligand-bound multiprotein complexes. Chem Biol 16(4):382–390
70. Salbo R, Bush MF, Naver H, Campuzano I, Robinson CV, Pettersson I, Jørgensen TJD, Haselmann KF (2012) Travelling-wave ion mobility mass spectrometry of protein complexes: accurate calibrated collision cross-sections of human insulin oligomers. Rapid Commun Mass Spectrom 26(10):1181–1193
71. Loo JA, Berhane B, Kaddis CS, Wooding KM, Xie Y, Kaufman SL, Chernushevich IV (2005) Electrospray ionization mass spectrometry and ion mobility analysis of the 20S proteasome complex. J Am Soc Mass Spectrom 16(7):998–1008
72. Ruotolo BT, Hyung S-J, Robinson PM, Giles K, Bateman RH, Robinson CV (2007) Ion mobility–mass spectrometry reveals long-lived, unfolded intermediates in the dissociation of protein complexes. Angew Chem Int Ed 46(42):8001–8004
73. Scott D, Layfield R, Oldham NJ (2015) Ion mobility–mass spectrometry reveals conformational flexibility in the deubiquitinating enzyme USP5. Proteomics 15(16):2835–2841
74. Smith DP, Giles K, Bateman RH, Radford SE, Ashcroft AE (2007) Monitoring copopulated conformational states during protein folding events using electrospray ionization-ion mobility spectrometry-mass spectrometry. J Am Soc Mass Spectrom 18(12):2180–2190
75. Knapman TW, Valette NM, Warriner SL, Ashcroft AE (2013) Ion mobility spectrometry-mass spectrometry of intrinsically unfolded proteins: trying to put order into disorder. Curr Anal Chem 9(2):181–191

76. Jurneczko E, Cruickshank F, Porrini M, Nikolova P, Campuzano Iain DG, Morris M, Barran PE (2012) Intrinsic disorder in proteins: a challenge for (un)structural biology met by ion mobility–mass spectrometry. Biochem Soc Trans 40(5):1021–1026
77. Pagel K, Natan E, Hall Z, Fersht AR, Robinson CV (2013) Intrinsically disordered p53 and its complexes populate compact conformations in the gas phase. Angew Chem Int Ed 52(1):361–365
78. Zhou M, Politis A, Davies RB, Liko I, Wu K-J, Stewart AG, Stock D, Robinson CV (2014) Ion mobility–mass spectrometry of a rotary ATPase reveals ATP-induced reduction in conformational flexibility. Nat Chem 6(3):208–215
79. Shepherd DA, Holmes K, Rowlands DJ, Stonehouse NJ, Ashcroft AE (2013) Using Ion mobility spectrometry–mass spectrometry to decipher the conformational and assembly characteristics of the hepatitis B capsid protein. Biophys J 105(5):1258–1267
80. Pierson NA, Chen L, Valentine SJ, Russell DH, Clemmer DE (2011) Number of solution states of bradykinin from ion mobility and mass spectrometry measurements. J Am Chem Soc 133(35): 13810–13813
81. Shi L, Holliday AE, Bohrer BC, Kim D, Servage KA, Russell DH, Clemmer DE (2016) "Wet" Versus "Dry" folding of polyproline. J Am Soc Mass Spectrom 1–11
82. Shi L, Holliday AE, Glover MS, Ewing MA, Russell DH, Clemmer DE (2015) Ion mobility-mass spectrometry reveals the energetics of intermediates that guide polyproline folding. J Am Soc Mass Spectrom 27(1):22–30
83. Shi L, Holliday AE, Shi H, Zhu F, Ewing MA, Russell DH, Clemmer DE (2014) Characterizing intermediates along the transition from polyproline i to polyproline II using ion mobility spectrometry-mass spectrometry. J Am Chem Soc 136(36): 12702–12711
84. Valentine SJ, Anderson JG, Ellington AD, Clemmer DE (1997) Disulfide-intact and -reduced lysozyme in the gas phase: conformations and pathways of folding and unfolding. J Phys Chem B 101(19):3891–3900
85. Niu S, Ruotolo BT (2015) Collisional unfolding of multiprotein complexes reveals cooperative stabilization upon ligand binding. Protein Sci 24(8):1272–1281
86. Hopper JTS, Oldham NJ (2009) Collision induced unfolding of protein ions in the gas phase studied by ion mobility-mass spectrometry: the effect of ligand binding on conformational stability. J Am Soc Mass Spectrom 20(10):1851–1858
87. Zhong Y, Han L, Ruotolo BT (2014) Collisional and coulombic unfolding of gas-phase proteins: high correlation to their domain structures in solution. Angew Chem Int Ed 53(35):9209–9212
88. Fernandez-Lima FA, Kaplan DA, Park MA (2011) Note: Integration of trapped ion mobility spectrometry with mass spectrometry. Rev Sci Instrum 82(12):126106
89. Fernandez-Lima F, Kaplan DA, Suetering J, Park MA (2011) Gas-phase separation using a trapped ion mobility spectrometer. Int J Ion Mobil Spectrom Off Publ Int Soc Ion Mobil Spectrom 14(2–3):93–98
90. Hernandez DR, Debord JD, Ridgeway ME, Kaplan DA, Park MA, Fernandez-Lima F (2014) Ion dynamics in a trapped ion mobility spectrometer. Analyst 139(8):1913–21
91. Schenk ER, Mendez V, Landrum JT, Ridgeway ME, Park MA, Fernandez-Lima F (2014) Direct observation of differences of carotenoid polyene chain cis/trans isomers resulting from structural topology. Anal Chem 86(4):2019–24
92. Schenk ER, Ridgeway ME, Park MA, Leng F, Fernandez-Lima F (2014) Isomerization kinetics of AT hook decapeptide solution structures. Anal Chem 86(2):1210–4
93. Gonzalez WG, Ramos V, Diaz M, Garabedian A, Molano-Arevalo JC, Fernandez-Lima F, Miksovska J (2016) Characterization of the photophysical, thermodynamic, and structural properties of the terbium (III)–DREAM complex. Biochemistry 55(12):1873–1886
94. Liu FC, Kirk SR, Bleiholder C (2016) On the structural denaturation of biological analytes in trapped ion mobility spectrometry - mass spectrometry. Analyst
95. Ridgeway ME, Silveira JA, Meier JE, Park MA (2015) Microheterogeneity within conformational states of ubiquitin revealed by high resolution trapped ion mobility spectrometry. Analyst 140(20):6964–6972
96. Molano-Arevalo JC, Hernandez DR, Gonzalez WG, Miksovska J, Ridgeway ME, Park MA, Fernandez-Lima F (2014) Flavin adenine dinucleotide structural motifs: from solution to gas phase. Anal Chem 86(20):10223–30
97. McKenzie-Coe A, DeBord JD, Ridgeway M, Park M, Eiceman G, Fernandez-Lima F (2015) Lifetimes and stabilities of familiar explosive molecular adduct complexes during ion mobility measurements. Analyst 140(16):5692–9
98. Cui T, Wei S, Brew K, Leng F (2005) Energetics of binding the mammalian high mobility group protein HMGA2 to poly (dA-dT) 2 and poly (dA)-poly (dT). J Mol Biol 352(3):629–645
99. George SE, Su Z, Fan D, Means AR (1993) Calmodulin-cardiac troponin C chimeras. Effects of domain exchange on calcium binding and enzyme activation. J Biol Chem 268(33):25213–25220
100. Evans SV, Brayer GD (1990) High-resolution study of the three-dimensional structure of horse heart metmyoglobin. J Mol Biol 213(4):885–897
101. Bushnell GW, Louie GV, Brayer GD (1990) High-resolution three-dimensional structure of horse heart cytochrome c. J Mol Biol 214(2):585–595
102. Gutiérrez-Magdaleno G, Bello M, Portillo-Téllez MC, Rodríguez-Romero A, García-Hernández E (2013) Ligand binding and self-association cooperativity of β-lactoglobulin. J Mol Recognit 26(2):67–75
103. Vijay-Kumar S, Bugg CE, Cook WJ (1987) Structure of ubiquitin refined at 1.8Åresolution. J Mol Biol 194(3):531–544
104. Czerwinska I, Far J, Kune C, Larriba-Andaluz C, Delaude L, De Pauw E (2016) Structural analysis of ruthenium-arene complexes using ion mobility mass spectrometry, collision-induced dissociation, and DFT. Dalton Trans 45(15):6361–6370
105. Larriba C, Hogan CJ (2013) Ion mobilities in diatomic gases: measurement versus prediction with non-specular scattering models. J Phys Chem A 117(19):3887–3901
106. Larriba C, Hogan CJ (2013) Free molecular collision cross section calculation methods for nanoparticles and complex ions with energy accommodation. J Comput Phys 251:344–363
107. Larriba-Andaluz C, Fernández-García J, Ewing MA, Hogan CJ, Clemmer DE (2015) Gas molecule scattering & ion mobility measurements for organic macro-ions in He versus N 2 environments. Phys Chem Chem Phys 17(22):15019–15029
108. Ouyang H, Larriba-Andaluz C, Oberreit DR, Hogan CJ Jr (2013) The collision cross sections of iodide salt cluster ions in air via differential mobility analysis-mass spectrometry. J Am Soc Mass Spectrom 24(12):1833–1847
109. Mao Y, Ratner MA, Jarrold MF (1999) Molecular dynamics simulations of the charge-induced unfolding and refolding of unsolvated cytochrome c. J Phys Chem B 103(45):10017–10021
110. Onufriev A, Case DA, Bashford D (2003) Structural details, pathways, and energetics of unfolding apomyoglobin. J Mol Biol 325(3):555–567
111. Arteca GA, Tapia O (2004) On the nature of the unfolded state: competing mechanisms in the unfolding of anhydrous protein ions. Chem Phys Lett 383(5):462–468
112. Chen L, Shao Q, Gao Y-Q, Russell DH (2011) Molecular dynamics and ion mobility spectrometry study of model β-hairpin peptide, trpzip1. J Phys Chem A 115(17):4427–4435

113. Zakharova NL, Crawford CL, Hauck BC, Quinton JK, Seims WF, Hill HH Jr, Clark AE (2012) An assessment of computational methods for obtaining structural information of moderately flexible biomolecules from ion mobility spectrometry. J Am Soc Mass Spectrom 23(5):792–805
114. D'Atri V, Porrini M, Rosu F, Gabelica V (2015) Linking molecular models with ion mobility experiments. Illustration with a rigid nucleic acid structure. J Mass Spectrom 50(5):711–726
115. Hall Z, Politis A, Bush MF, Smith LJ, Robinson CV (2012) Charge-state dependent compaction and dissociation of protein complexes: insights from ion mobility and molecular dynamics. J Am Chem Soc 134(7):3429–3438
116. Breuker K, McLafferty FW (2008) Stepwise evolution of protein native structure with electrospray into the gas phase, 10–12 to 102 s. Proc Natl Acad Sci 105(47):18145–18152
117. Kebarle P, Tang L (1993) From ions in solution to ions in the gas phase-the mechanism of electrospray mass spectrometry. Anal Chem 65(22):972A–986A
118. Shi H, Atlasevich N, Merenbloom SI, Clemmer DE (2014) Solution dependence of the collisional activation of ubiquitin [M+ 7H] 7+ ions. J Am Soc Mass Spectrom 25(12):2000–2008
119. Vahidi S, Stocks BB, Konermann L (2013) Partially disordered proteins studied by ion mobility-mass spectrometry: implications for the preservation of solution phase structure in the gas phase. Anal Chem 85(21):10471–10478
120. Going CC, Williams ER (2015) Supercharging with m-nitrobenzyl alcohol and propylene carbonate: forming highly charged ions with extended, near-linear conformations. Anal Chem 87(7):3973–3980
121. Shi H, Pierson NA, Valentine SJ, Clemmer DE (2012) Conformation types of ubiquitin [M+ 8H] 8+ ions from water: methanol solutions: evidence for the N and A states in aqueous solution. J Phys Chem B 116(10):3344–3352
122. Castellanos A, Benigni P, Hernandez DR, DeBord JD, Ridgeway ME, Park MA, Fernandez-Lima F (2014) Fast screening of polycyclic aromatic hydrocarbons using trapped ion mobility spectrometry—mass spectrometry. Anal Methods Adv Methods Appl 6(23):9328–9332
123. Benigni P, Thompson CJ, Ridgeway ME, Park MA, Fernandez-Lima F (2015) Targeted high-resolution ion mobility separation coupled to ultrahigh-resolution mass spectrometry of endocrine disruptors in complex mixtures. Anal Chem 87(8):4321–5
124. Sobott F, Hernández H, McCammon MG, Tito MA, Robinson CV (2002) A tandem mass spectrometer for improved transmission and analysis of large macromolecular assemblies. Anal Chem 74(6):1402–1407
125. Adams KJ, Montero D, Aga D, Fernandez-Lima F (2016) Isomer separation of polybrominated diphenyl ether metabolites using nanoESI-TIMS-MS. Int J Ion Mobil Spectrom 1–8